Bull. Mater. Sci., Vol. 36, No. 3, June 2013, pp. 461–469. © Indian Academy of Sciences.

# Synthesis, IR, crystallization and dielectric study of (Pb, Sr)$TiO_3$ borosilicate glass–ceramics

**C R GAUTAM*, D KUMAR†, O PARKASH† and PRABHAKAR SINGH‡**

Department of Physics, University of Lucknow, Lucknow 226 007, India
†Department of Ceramic Engineering, ‡Department of Applied Physics, Institute of Technology, Banaras Hindu University, Varanasi 221 005, India

**Abstract.** **Eleven glass compositions were prepared by melt and quench method with progressive substitution of SrO for PbO ($0 \leq x \leq 1{\cdot}0$) with a step-wise increment of 0·10 in the glass $[(Pb_xSr_{1-x})OTiO_2]$–$[(2SiO_2B_2O_3)]$–$[BaO{\cdot}K_2O]{\cdot}Nb_2O_5$ (mol percentage) system. The infrared spectra (IR) of various glass compositions in the above mentioned glass system was recorded over a continuous spectral range 400–4000 $cm^{-1}$ to study their different oxides structure systematically. Differential thermal analysis (DTA) was recorded from room temperature (∼27 °C) to 1400 °C employing a heating rate of 10 °C/min to determine glass transition temperature, $T_g$ and crystallization temperature, $T_c$. The melting temperature, $T_m$, of these glass compositions was found to be in the range 597–1060 °C depending on the composition under normal atmospheric conditions. $T_g$ and $T_m$ of glasses were found to increase with increasing SrO content. X-ray diffraction analysis of these glass–ceramic samples shows that major crystalline phase of the glass–ceramic sample with $x \leq 0{\cdot}5$ was found to have cubic structure similar to $SrTiO_3$ ceramic. Scanning electron microscopy has been carried out to see the surface morphology of the crystallites dispersed in the glassy matrix.**

**Keywords.** **(PbSr)$TiO_3$ borosilicate glasses; infrared spectroscopy; DTA; XRD and SEM.**

## 1. Introduction

Study of various oxide glasses has received considerable attention due to their structural properties (Kamitos and Karakassides 1989; Motke *et al* 2002). These glasses have wide applications in the fields of electronics, nuclear, solar energy technologies and acoustic–optics devices (Hirashima *et al* 1985; Khanna *et al* 1996; Rajendran *et al* 1999; Singh *et al* 2002). The structural and physical properties of PbO glasses have been described well by Worrel and Henshell (1978). PbO can enter a glass network both as a network former and as a network modifier (Motke *et al* 2002). At lower concentrations, PbO modifies the network through forming $BO_4$ tetrehedra at the rate of two $BO_4$ groups per PbO molecule (Doweider *et al* 1991) and at higher concentrations; PbO can partly play the role of a glass forming oxide in the form of $PbO_4$ pyramids with $Pb^{2+}$ at the apex of the pyramid (Bray *et al* 1963). Sahu *et al* (2003a) demonstrated the crystallization of solid solution ferroelectric $Pb_{1-x}Sr_xTiO_3$ in borosilicate–glassy matrix with the help of DTA and XRD studies. He also demonstrated that addition of varying ratios of alkali oxide, $K_2O$ to alkaline-earth oxide, BaO influences the ease of formation of glass and its crystallization behaviour (Thakur *et al* 1997; Sahu *et al* 2006). Gautam *et al* (2010) have investigated IR study of Pb–Sr titanate borosilicate glasses and reported that absorption of IR peaks occurs due to different vibrational modes of the borate network of which asymmetric stretching relaxation of B–O bond of trigonal $BO_3$ units contribute alone. He also reported that low frequency band in IR spectra can be attributed to vibration of metal cation such as $Pb^{2+}$. Gautam *et al* (2011a) have investigated crystallization behaviour and microstructural analysis of lead-rich and strontium-rich $(Pb_xSr_{1-x})TiO_3$ (PST) glass–ceramics system containing 1 mole% $La_2O_3$ and explored the possibility to crystallize the desired $PbTiO_3$ (PT) and PST phase in the glassy matrix. More recently, Gautam *et al* (2011b) have reported results of the investigation on dielectric and impedance spectroscopic studies of $(Sr_{1-x}Pb_x)TiO_3$ glass–ceramics with addition of $Nb_2O_5$ and found very good crystallization and high value of dielectric constant. The high value of relative dielectric constant was found due to the addition of $Nb_2O_5$, because it enhanced the crystallization of the parent glasses. In the present work, an attempt has been made to undertake a structural and crystallization investigation of glass $[(Pb_xSr_{1-x})OTiO_2]$–$[(2SiO_2B_2O_3)]$–$[BaO{\cdot}K_2O]{\cdot}Nb_2O_5$ system with the help of IR, DTA, XRD and SEM characterization.

## 2. Experimental

### 2.1 *Sample preparation*

Glass samples of different compositions in glass $[(Pb_xSr_{1-x})OTiO_2]$–$[2SiO_2B_2O_3]$–$[K_2O]$–$[BaO]$–$[Nb_2O_5]$ system with $x = 0{\cdot}0$–$1{\cdot}0$ mole fraction were prepared. The

*Author for correspondence (gautam_ceramic@yahoo.com)

raw materials of PbO, $SrCO_3$, $TiO_2$, $SiO_2$, $H_3BO_3$, $BaCO_3$, $K_2CO_3$ and $Nb_2O_5$ of AR grade were obtained from Aldrich, Glaxo and CDH Chemical Company. Appropriate amounts of chemicals were weighed by using a digital balance with an accuracy of 0·0001 g. The weighed chemicals were thoroughly mixed in an agate mortar and pestle in acetone media until they were dried. The dry powders were melted in high-pure alumina crucible in the temperature range 1120–1290 °C for 1 h until a bubbled-free liquid was formed. The melt was then poured into a pre-heated aluminum mold, pressed by a thick aluminum plate. The mold was then moved into an annealing furnace at an annealing temperature of 300 °C for 3 h to avoid breaking the glass sample through residual internal strain.

### 2.2 *Infrared spectra*

Infrared spectroscopy was carried out at room temperature in the region from 400 to 4000 $cm^{-1}$ using Bruker FTIR Tensor-27. Each powder sample weighing 5 mg was mixed with 25 mg of KBr powder in an agate mortar and then pressed into pellets form. The pellets were used for recording the absorption spectra. In our PST borosilicate–glass system, some of the glass compositions depict change in the glass structure. The various bands are recorded with respect to different stretching modes of vibrations.

### 2.3 *Differential thermal analysis (DTA)*

Differential thermal analysis (DTA) studies of sugar-like powdered glasses were conducted using a NETZSCH simultaneous thermal analyser (STA-409) from room temperature to 1200 °C employing a heating rate of 10 °C/min. About 50 mg of glass powder was used for thermal analysis studies. Sintered kaolin was used as reference material. The evolution or absorption of heat accompanies with chemical reactions or structural changes within glass samples. The process of crystallization in glasses is an exothermic process since the free energy of the crystalline phase is lower than that of glassy phase. If DTA run is made on a sample of glass which devitrifies on heating, a number of exothermic peaks will be observed corresponding to the separation of different crystalline phases. Hence, DTA pattern, crystallization temperature, $T_c$, for the possible crystalline phases were determined. In addition to $T_c$, the annealing temperature and glass transition temperature, $T_g$, can also be determined from DTA patterns.

### 2.4 *X-ray diffraction (XRD)*

X-ray powder diffraction patterns were recorded employing a Rigaku ID 3000 diffractometer using Cu$K\alpha$ radiation. The crystalline phase in each glass–ceramic sample were identified by comparing its XRD with PDF–JCPDS standard powder diffraction patterns of various crystalline phases, which might have formed from different constituent oxides of the glass. A systematic study of the presence of various crystalline phases in glass–ceramic samples with respect to their heat treatment schedule helps in understanding the crystallization behaviour of different glasses. Crystal structure was determined by using Cell software.

### 2.5 *Scanning electron microscopy (SEM)*

Scanning electron microscopy (SEM) is one of the most versatile instruments available for the examination and analysis of the microstructural characteristics of solid objects. The glass–ceramic samples were ground and polished successively using SiC powders (mesh nos 120, 200, 400 and 1000) on a flat glass plate. The final polishing was done on a blazer cloth using diamond paste (1 $\mu$m) and Hiffin fluid. The polished samples were etched for approximately 1 min with a 30% $HNO_3$ + 20% HF solution to delineate the morphology of crystallites and their distribution. The etched samples were cleaned thoroughly with distilled water. Samples were prepared for SEM examination by sputtering silver–palladium alloy or gold films onto the etched surfaces of glass–ceramics to prevent charge build up. The samples were then examined using a JSM-840 scanning electron microscope. The glass–ceramic samples were mounted on the stubs with Ag-conducting paint and photographs were recorded at a magnification of 1500, 5000, 8000 and 2500×.

### 2.6 *Dielectric measurements*

Both the surfaces of glass–ceramic samples were ground and polished using SiC powders (mesh nos 200, 400 and 1000) for attaining smooth surface for a thickness of about 1 mm. The electrodes were made by applying silver paint (code no. 1337-A, Elteck Corporation, India) on both the sides of the polished glass–ceramic samples and cured at 700 °C for 10 min. The capacitance measurement was made by heating the sample in a locally fabricated sample holder using an automated measurement system. The sample was mounted on a locally-fabricated sample holder, which was kept in a programmable heating chamber. This heating chamber is a part of the dielectric measurement setup. The electrodes of the sample holder are connected to HP 4284A precision LCR meter through scanner relay boards and HPIB bus which in turn is connected to a computer and a printer. Measurements of operational controls and data recording are done through the computer. The sample was heated in the heating chamber to required temperature at a rate of 2 °C/min. Curie temperature of $(Pb_{1-x}Sr_x)TiO_3$ ceramic ranges from below room temperature to 490 °C. Capacitance and dissipation factor of glass–ceramic sample were recorded at 0·1, 1, 10, 100 kHz and 1 MHz at an interval of 2 °C. Dielectric constant ($\varepsilon_r$) was calculated from the measured capacitance ($C$) using the following equation:

$$\varepsilon_r = \frac{C \times d}{\varepsilon_0 A}, \tag{1}$$

where $C$ is the capacitance, $\varepsilon_0$ the permittivity of free space ($8{\cdot}854 \times 10^{-12}$ F/m), $d$ the thickness (m) and $A$ the area ($m^2$) of the sample. The dielectric constant and dissipation factor were plotted as a function of temperature at a few selected frequencies to show the variation of dielectric constant with temperature and frequency of applied electric field.

Dissipation factor was noted directly or calculated by using the following relation:

$$D = \frac{G}{\omega C}, \tag{2}$$

where $\omega = 2\pi f$, $f$ is the frequency and $G$ the conductance.

### 2.7 *Nomenclature of glass and glass–ceramic samples*

Five letters glass code has been adapted to the composition of all the glasses. The first two letters PT, 9P, etc represent the fraction of lead, i.e. $x$ in the glass. PT refers to $x = 1{\cdot}0$, i.e. 100% PbO and 0% SrO. 9P, 8P, etc refers to $x = 0{\cdot}9$, $0{\cdot}8$, respectively. The third letter N indicates that $Nb_2O_5$ is used as an additive. The last two letters 5B refer to fraction of modifier oxides BaO in the parent glass compositions. The last letter indicates the crystallization time in hours, i.e. S stands for 6 h.

## 3. Results and discussion

### 3.1 *Infrared spectroscopic study of glasses*

Infrared absorption spectra of the glasses under investigation have been recorded in order to obtain information about the possible changes of vibrational spectra. These vibrational spectra are due to the process of structural grouping rearrangements with a change in glass composition. Important changes in the properties of glass can occur as a result of structural transformations (Kumar *et al* 1997). $B_2O_3$ is a well known network former with $BO_3$ structural units. The presence of $BO_4$ units are evident in these glasses from the study of IR spectra. Infrared spectra for all the glasses are shown in figures 1 and 2, respectively. IR spectra of these glasses consist of broad and sharp bands in different regions (400–4000 $cm^{-1}$). These bands are strongly affected by increasing substitution of Sr for Pb. Wavenumbers of different absorption peaks for all the glasses are listed in table 1. All the absorption peaks have been numbered as 1, 2, ..., 8, starting from high wavenumber side to low wavenumber side (table 2). Infrared spectra of these glasses show eight absorption peaks. The peaks are sharp, medium and broad in nature. The first absorption peak lies in the range 3445–3481 $cm^{-1}$. This peak is broad in Pb-rich glass samples while it is sharp in Sr-rich glass samples. This broad absorption peak is attributed to hydroxyl or water group (Adams and Douglas 1959). Peak no. 2 splits into two absorption peaks, i.e. 2 (a and b). Both the peaks are very close to each other as shown in table 1. This peak is due to the hydrogen bonding. Dunken and Doremus (1987) and

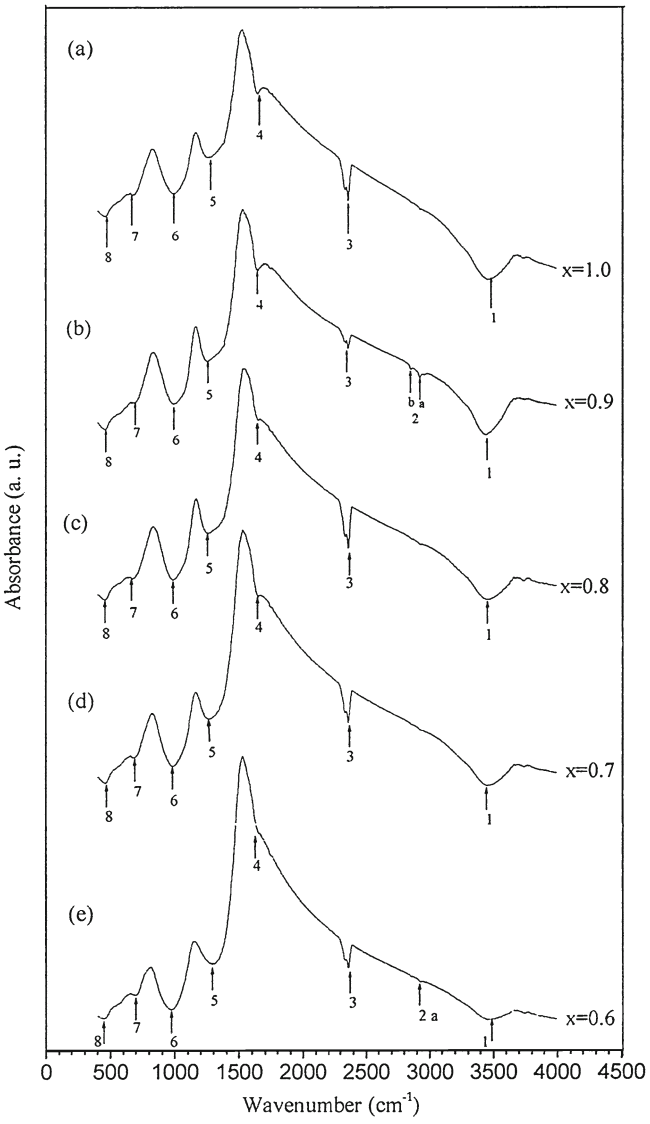


**Figure 1.** Infrared spectra of glasses: (**a**) PTN5B, $x = 1{\cdot}0$; (**b**) 9PN5B, $x = 0{\cdot}9$; (**c**) 8PN5B, $x = 0{\cdot}8$; (**d**) 7PN5B, $x = 0{\cdot}7$ and (**e**) 6PN5B, $x = 0{\cdot}6$.

Husung and Doremus (1990) have divided the broad water bands into: (a) peak 2700–3000 $cm^{-1}$, originating from hydrogen bonding; (b) peak 3200–3500 $cm^{-1}$, originating from molecular water and (c) peak 3600–3750 $cm^{-1}$, originating from OH– groups. Absorption peak no. 3 is absent in intermediate compositions, $x = 0{\cdot}5$ and $0{\cdot}4$ while it is present in rest of the glass compositions. In this glass system, closely lying peaks at 1338, 1352 $cm^{-1}$ show presence of pyroborate, orthoborate and all the borate groups containing $BO_3$ units (Chekhovskii 1985). Two broad absorption peak nos 4 and 5 are observed in all the glass compositions with $x = 1$–0. Peak no. 5 splits into two peaks with glass compositions, $x = 0{\cdot}3$, $0{\cdot}2$ and 0, which are rich in Sr (figure 3(c, d and e)). These absorption peaks occur due to the vibrational mode of the borate network. The vibrational modes of the borate network are mainly due to the asymmetric stretching relaxation of the B–O bond of trigonal $BO_3$ units. These

vibrational modes occur at 1200–1600 $cm^{-1}$ (Kamitos *et al* 1987; Ezz Eldin *et al* 1995; Ghoneun *et al* 1996; Gautam *et al* 2010). A broad absorption peak no. 6 appeared in all IR spectra of the glass samples. This broad absorption peak lies between 954 and 1000 $cm^{-1}$ and is due to B–O–B linkage, in which both boron atoms are tetrahedrally coordinated and triborate super-structural unit (Singh *et al* 1989). It is clearly observed from IR spectra that with the replacement of SrO by PbO content, bands shifted to 1000, 997, 987, 985 and 968 $cm^{-1}$ in the glass samples, PTN5B, 9PN5B, 8PN5B, 7PN5B and 6PN5B, respectively. Absorption bands at around 1000 $cm^{-1}$ peak (no. 6) are attributed to a stretching vibration of B–O–Si linkage (Tenny and Wong 1972). A broad absorption peak (no. 7) is observed in all the IR spectra. This peak lies between 671 and 709 $cm^{-1}$ and is due to the bending of B–O–B linkages in the borate glassy network (Doweider *et al* 1991; Gautam *et al* 2010). Wavenumber of this peak increases with increasing concentration of SrO (table 1). The absorption peak (no. 8) at around 420 $cm^{-1}$ is due to the vibration of cations such as $Pb^{2+}$ and $Sr^{2+}$ (Motke *et al* 2002), and hence network modifying behaviour is observed in which these ions enter the interstices on the network (Singh *et al* 2008). The same band is also present in $PbO–B_2O_3$ glass and is attributed to the vibrations of $Pb^{2+}$ cations (Bray and Keefe 1963).

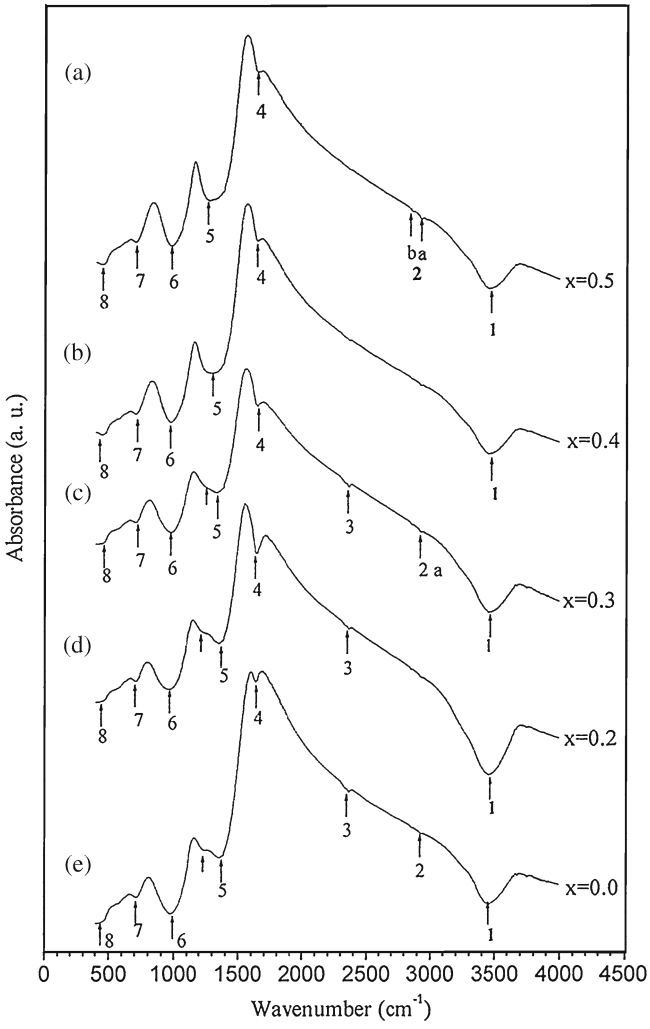


**Figure 2.** Infrared spectra of glasses: (**a**) 5PN5B, $x = 0{\cdot}5$; (**b**) 4PN5B, $x = 0{\cdot}4$; (**c**) 3PN5B, $x = 0{\cdot}3$; (**d**) 2PN5B, $x = 0{\cdot}2$ and (**e**) STN5B, $x = 0{\cdot}0$.

### 3.2 *Differential thermal analysis (DTA) studies*

DTA patterns of some representative glasses in the system $[(Pb_xSr_{1-x})OTiO_2]–[(2SiO_2B_2O_3)]–[BaO{\cdot}K_2O]–Nb_2O_5$ are shown in figures 3(a–c) and 4(a and b). These DTA patterns show a shift in the base line at a temperature in the range 590–670 °C. The shifts in the base line representing a change in the specific heat may be attributed to the glass transition temperature (Sahu *et al* 2003b). The glass code, glass transition temperatures, $T_g$ and crystallization temperature, $T_c$ for different glass compositions are listed in table 3. It is observed from the table that $T_g$ increases with increasing concentration of SrO. The increase in $T_g$ is due to the increasing viscosity of the melt with increasing SrO concentration. Figure 3(a–c) represents DTA patterns for the glass samples 4PN5B, 3PN5B and 2PN5B, respectively.

**Table 1.** Wavelengths of different absorption peaks in IR spectra of the glasses in $[(Pb_xSr_{1-x})OTiO_2]–[(2SiO_2B_2O_3)]–[BaO{\cdot}K_2O]–Nb_2O_5$ system.

| | | Wavelength of different absorption peaks ($cm^{-1}$) | | | | | | | | |
|---|---|---|---|---|---|---|---|---|---|---|
| | | | 2 | | | | | | | |
| Glass codes | $x$ | 1 | *A* | *b* | 3 | 4 | 5 | 6 | 7 | 8 |
| PTN5B | 1·0 | 3481 | – | – | 2363 | 1641 | 1265 | 1000 | 685 | 463 |
| 9PN5B | 0·9 | 3445 | 2924 | 2854 | 2360 | 1647 | 1257 | 997 | 688 | 457 |
| 8PN5B | 0·8 | 3452 | – | – | 2361 | 1652 | 1261 | 987 | 671 | 461 |
| 7PN5B | 0·7 | 3452 | – | – | 2362 | 1649 | 1267 | 985 | 673 | 461 |
| 6PN5B | 0·6 | 3452 | 2927 | – | 2364 | 1658 | 1292 | 968 | 694 | 451 |
| 5PN5B | 0·5 | 3454 | 2925 | 2856 | – | 1649 | 1275 | 987 | 702 | 449 |
| 4PN5B | 0·4 | 3473 | – | – | – | 1649 | 1286 | 954 | 704 | 455 |
| 3PN5B | 0·3 | 3456 | 2937 | – | 2362 | 1649 | 1338 | 968 | 704 | 420 |
| 2PN5B | 0·2 | 3454 | – | – | 2362 | 1647 | 1352 | 956 | 706 | 453 |
| STN5B | 0·0 | 3448 | 2937 | – | 2361 | 1635 | 1244 | 987 | 709 | 415 |

**Table 2.** Wavenumber assignment of infrared absorption band of studied glasses.

| No. of peaks | Peak position ($cm^{-1}$) | Assignment |
|---|---|---|
| 1 | 3600–3750 | OH group |
| 2 | 3200–3500 | Molecular water |
| 3 | 2700–3000 | Hydrogen bonding |
| 4 | 1338, 1348 | Presence of pyroborate, orthoborate and groups containing $BO^{3-}$ units |
| 5 | 1250–1500 | $BO_3$ stretching |
| 6 | 964 | B–O–B linkage |
| 7 | 708 | $BO_4$ stretching |
| 8 | 420 | Vibrations of metal cations such as $Pb^{2+}$, $Sr^{2+}$ |

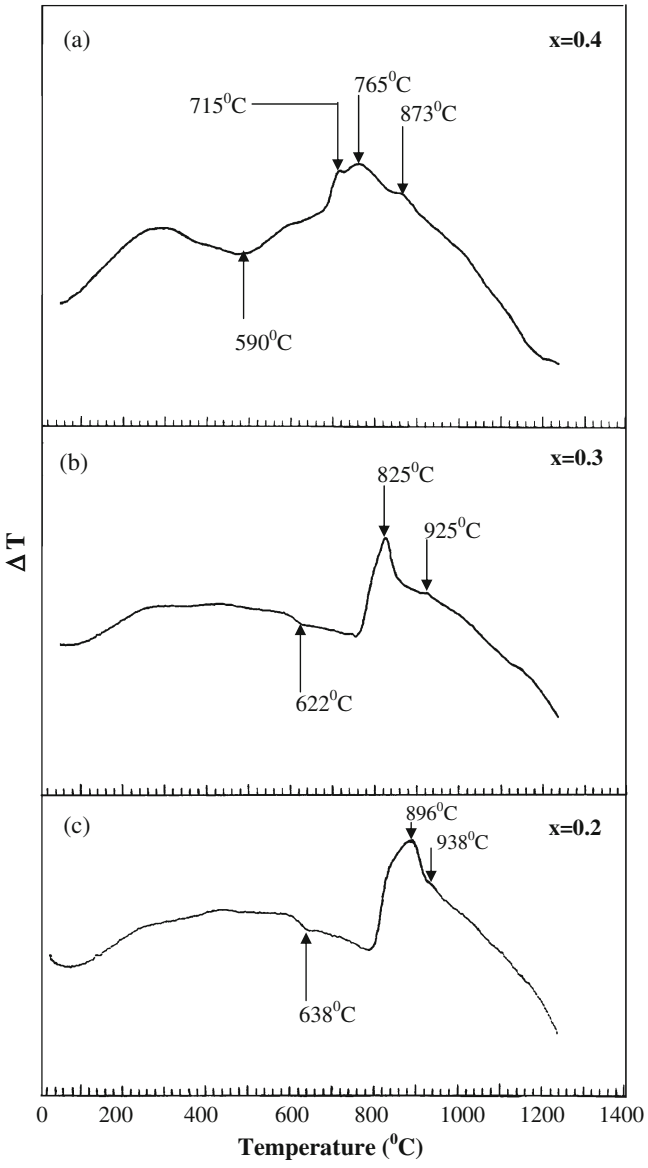


**Figure 3.** DTA patterns of: (**a**) 4PN5B, (**b**) 3PN5B and (**c**) 2PN5B glass samples.

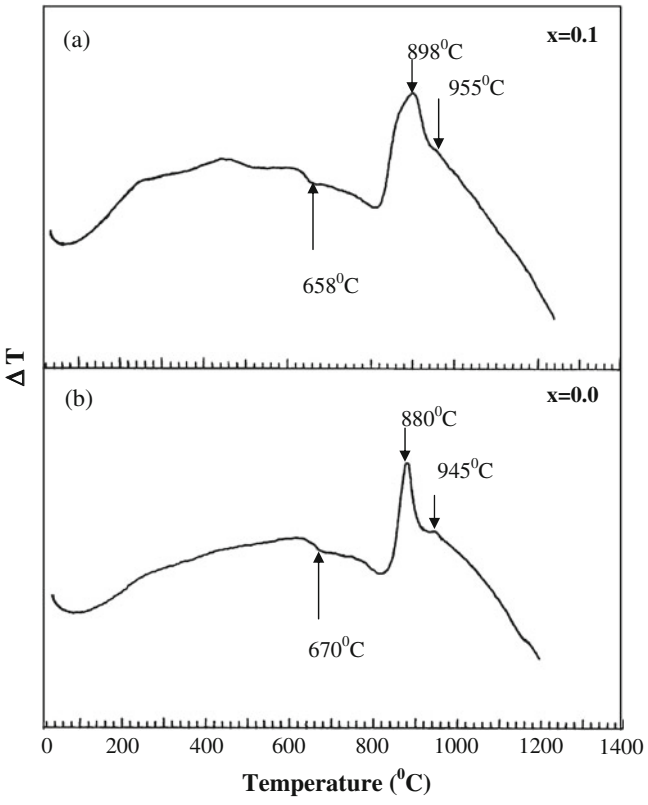


**Figure 4.** DTA patterns of: (**a**) 1PN5B and (**b**) STN5B glass samples.

Three exothermic peaks $T_{c1}$, $T_{c2}$ and $T_{c3}$ are observed for glass sample 4PN5B around 715, 765 and 873 °C, respectively. Peak $T_{c2}$ is due to the major phase formation of perovskite, PST, while peaks $T_{c1}$ and $T_{c3}$ are due to secondary phases. DTA pattern of glass sample 3PN5B ($x = 0{\cdot}3$) shows two exothermic peaks, first peak is sharp at 825 °C, while second peak appears as a shoulder at 925 °C. The first sharp peak is due to the exothermic reaction for formation of perovskite titanate phase. The second peak $T_{c3}$ at 925 °C may be attributed to the crystallization of secondary phase of lead borate, $PbB_2O_4$ (PB) or trace amount of strontium borate, $Sr_2B_2O_5$ (SB). It may also be due to the recrystallization of the glass–ceramic samples.

DTA patterns for the glass samples 1PN5B and STN5B ($x = 0{\cdot}1$–$0{\cdot}0$) showed only two exothermic peaks $T_{c3}$ and $T_{c4}$ at around 898, 955, 880 and 945 °C, respectively (figure 4). A single sharp peak, $T_{c3}$, in their DTA patterns is the signature of the good crystallization of these

**Table 3.** Glass transition temperature and DTA peaks of various glass samples in system $[(Pb_xSr_{1-x})TiO_2]$–$[2SiO_2{\cdot}B_2O_3]$–$[BaO{\cdot}K_2O]$–$[Nb_2O_5]$.

| Composition, $x$ | Glass code | DTA peaks (°C) | | | | |
|---|---|---|---|---|---|---|
| | | $T_g$ | $T_{c1}$ | $T_{c2}$ | $T_{c3}$ | $T_{c4}$ |
| 0·4 | 4PN5B | 590 | – | 715 | 765 | 873 |
| 0·3 | 3PN5B | 622 | – | – | 825 | 925 |
| 0·2 | 2PN5B | 638 | – | – | 896 | 938 |
| 0·1 | 1PN5B | 658 | – | – | 898 | 955 |
| 0·0 | STN5B | 670 | – | – | 880 | 945 |

glasses with desired phase of perovskite–strontium titanate (ST). From the X-ray diffraction studies of various glass–ceramic samples it appears that single exothermic peak in DTA plot corresponds to the crystallization of PST/ST phases. It is concluded that the addition of $Nb_2O_5$ acts as a nucleating agent and hence it promotes good crystallization in Sr-rich compositions. It is also concluded that the lead-rich compositions did not give good crystallization and also led to crystallization of secondary phase formation of $PbTi_3O_7$ in large content (Gautam *et al* 2011a, b). This is shown by X-ray diffraction of these glass–ceramic samples. From X-ray diffraction studies of the glass–ceramic samples, it appears that single exothermic peak in DTA plot corresponds to the crystallization of ST phase (Gautam 2005). It is observed from DTA patterns that the shifting takes place towards the higher temperature side for $T_g$, as well as in $T_c$, which is in good agreement with shifting in the absorption peaks of IR patterns.

### 3.3 *XRD analysis*

Figure 5 shows XRD pattern for the glass–ceramic composition $x = 0{\cdot}4$ and 0·3. Glass–ceramic sample 4PN5B715S was obtained by the crystallization of glass sample 4PN5B at 715 °C for 6 h. XRD pattern of this glass–ceramic sample shows PST as major phase with an unidentified phase as secondary phase. Glass sample 3PN5B was crystallized at two different temperatures on the basis of their DTA exothermic peaks $T_{c3}$ and $T_{c4}$ for 6 h. Trace amount of rutile (R) and unidentified phase of glass–ceramic sample 3PN5B825S were observed. On further raising the crystallization temperature from 825 to 925 °C, secondary phase changed from R to SB as shown in XRD patterns of these glass–ceramic samples. The observed phases are listed in table 4. Figure 6 shows XRD patterns of various glass–ceramic samples with $x = 0{\cdot}2$–0·0. All the glass–ceramic samples were prepared for 6 h soaking time. XRD pattern of the glass–ceramic sample 2PN5B896S shows trace amount of secondary phase of R. Glass–ceramic sample 1PN5B898S ($x = 0{\cdot}1$) was obtained by the crystallization of the glass 1PN5B at 896 °C for 6 h. XRD pattern of this glass–ceramic sample shows major phase of PST with secondary phase of SB. Lead free glass–ceramic sample STN5B880S was obtained by the crystallization of the glass sample STN5B at 880 °C for 6 h. XRD

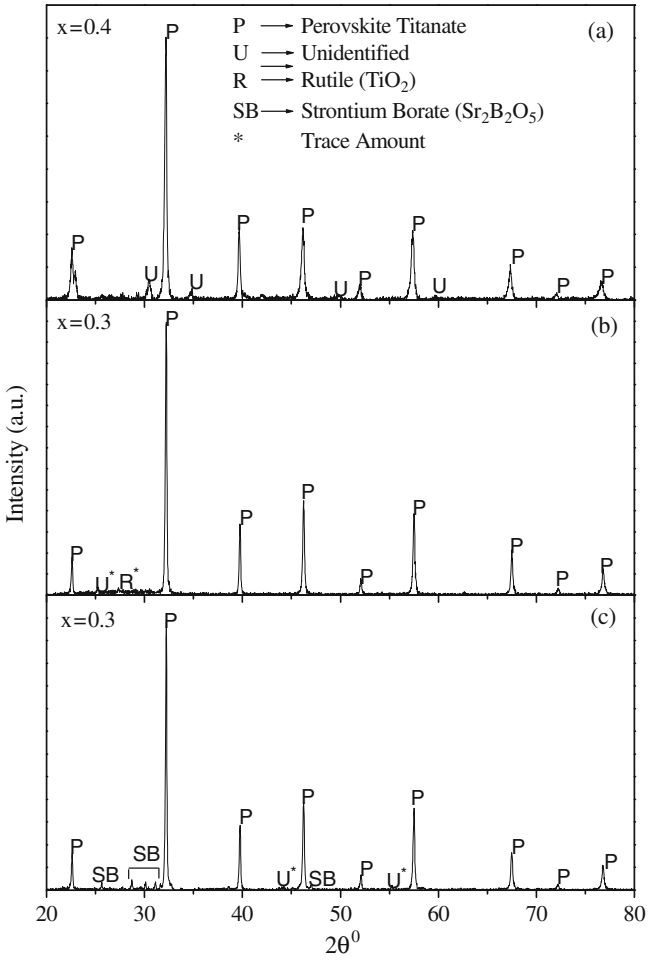


**Figure 5.** X-ray diffraction patterns of different glass–ceramic samples: (**a**) 4PN5B765S; (**b**) 3PN5B825S and (**c**) 3PN5B925S in system $[(Pb_xSr_{1-x})OTiO_2]$–$[(2SiO_2B_2O_3)]$–$[BaO{\cdot}K_2O]-Nb_2O_5$.

pattern of this glass–ceramic sample is shown in figure 6(c). From XRD pattern, it is observed that major phase of ST is crystallized along with secondary phases of R and SB.

### 3.4 *Surface morphology*

Figure 7(a–f) shows scanning electron micrographs for glass–ceramic samples 4PN5B765S, 3PN5B825S, 2PN5B896S, 1PN5B898S and STN5B880S crystallized for

**Table 4.** Heat treatment schedules, glass–ceramic codes and crystalline phases of different strontium-rich glass–ceramic samples in system $[(Pb_xSr_{1-x})OTiO2]$–$[2SiO_2{\cdot}B_2O_3]$–$[K_2O]$–[BaO]–$[Nb_2O_5]$.

| Glass code | Glass–ceramic code | Heat treatment schedules | | | Crystalline phases |
|---|---|---|---|---|---|
| | | Heating rate (°C/min) | Holding temp. (°C) | Holding time (h) | |
| 4PN5B | 4PN5B765S | 5 | 765 | 6 | P+SB+U* |
| 3PN5B | 3PN5B825S | 5 | 825 | 6 | P+R*+U* |
| | 3PN5B925S | 5 | 925 | 6 | P+SB+U* |
| 2PN5B | 2PN5B896S | 5 | 896 | 6 | P+R* |
| 1PN5B | 1PN5B898S | 5 | 898 | 6 | P+SB |
| STN5B | STN5B880S | 5 | 880 | 6 | P+R*+SB |

*Note*: P – Perovskite titanate; SB – Strontium borate ($Sr_2B_2O_5$); R – rutile ($TiO_2$); U – unidentified; * – trace amount.

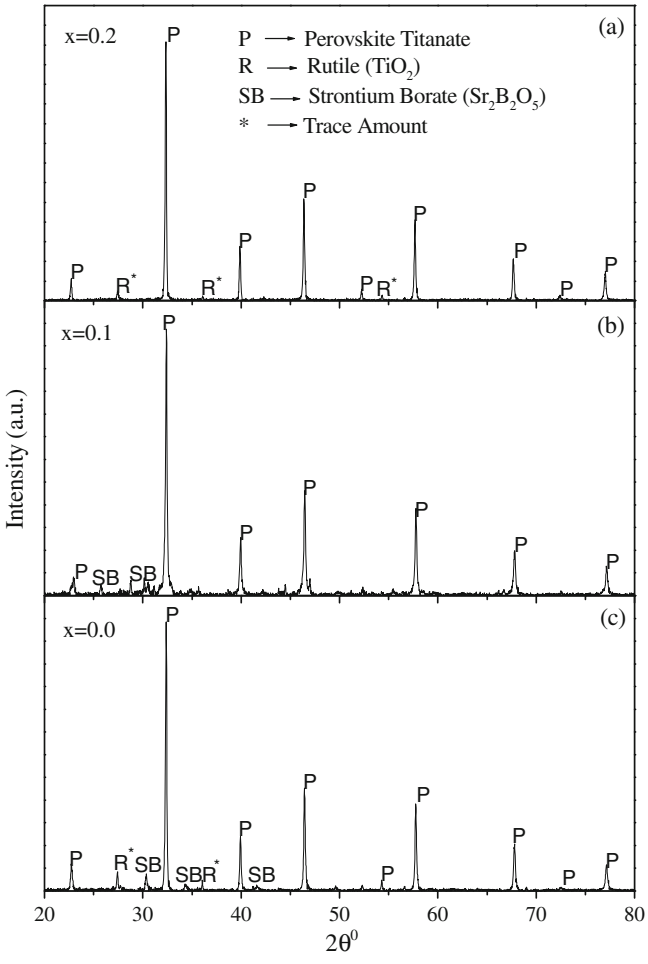


**Figure 6.** X-ray diffraction patterns of different glass–ceramic samples: (**a**) 2PN5B896S, (**b**) 1PN5B898S and (**c**) STN5B880S in system $[(Pb_xSr_{1-x})OTiO_2]$–$[(2SiO_2B_2O_3)]$–$[BaO{\cdot}K_2O]-Nb_2O_5$.

6 h, respectively. In the glass–ceramic sample, 4PN5B765S, major phase of perovskite PST with enhanced crystal growth, connectivity and uniform distribution in the glassy matrix were observed. These crystallites of major phase are very fine having size of the order of submicrons. Figure 7(b and c) shows scanning electron micrographs for glass–ceramic samples 3PN5B825S and 2PN5B896S for 6 h at high magnifications. Directional and chain-like morphology of the crystallites were observed for glass–ceramic sample 3PN5B825S while it is randomly observed and interconnected to each other for 2PN5B896S. The secondary phase of R, which is more shining in comparison to the major phase, is seen in SEM of this sample at high magnification. Figure 7(e and f) shows SEM for glass–ceramic samples, 1PN5B898S and STN5B880S. Major phase of perovskite, ST, was observed for both glass–ceramic samples. Spherulitic crystal growth of major phase of ST is observed while the white tiny crystallites of secondary phase of R are observed. All spherulites comprise fibrous crystals radiating from a common centre. Most of these have a spherical shape, but a few have a sheaf-like appearance (Keith and Padden 1963). Good crystallization is observed for these glass–ceramic samples. This is confirmed on the basis of XRD and SEM studies. The secondary phase of SB and R are clearly seen in the micrograph of glass–ceramic sample STN5B880S.

### 3.5 *Dielectric behaviour*

The variation of dielectric constant, $\varepsilon_r$ and dissipation factor, $D$, for 1PN5B898S glass–ceramic samples in the present system are shown in figure 8. Dielectric behaviour of this glass–ceramic sample shows very small temperature dependence of dielectric constant at 0·1, 1 and 10 kHz frequencies while it is temperature independent at higher frequencies such as 100 kHz and 1 MHz. Increase in $\varepsilon_r$ and $D$ may be due to increase in electrical conduction with increasing temperature. The dielectric behaviour of this glass–ceramics can be explained as follows: addition of $Nb_2O_5$ promotes crystallization of glass during heat treatment. Nb acts as donor dopant in $(PbSr)TiO_3$. When glass–ceramic sample is crystallized at higher temperatures, Nb ions present in the glass diffuse into the crystalline perovskite phase of ST and make it semiconducting. It can also change Curie temperature. On the application of electric field, glass–ceramic sample 1PN5B898S shows space charge polarization around the semiconducting crystal and insulating glass interface giving rise to very high value of dielectric constant. The space charge polarization relaxes with increasing frequency. The

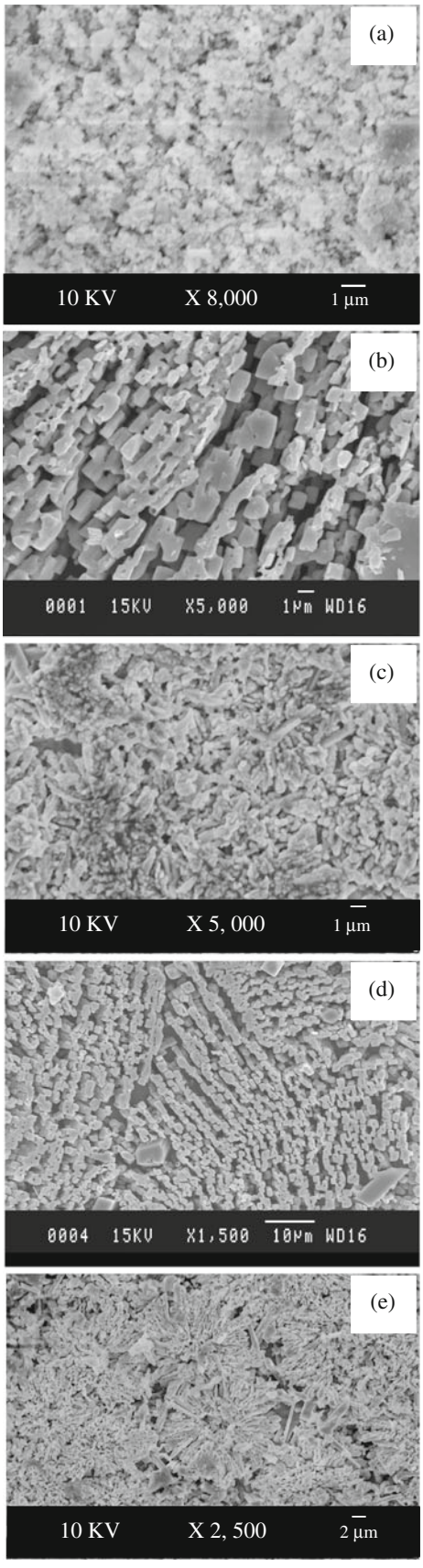


**Figure 7.** Scanning electron micrographs of polished and chemically-etched surfaces of glass–ceramic sample: (**a**) 4PN5B765S; (**b**) 3PN5B825S; (**c**) 2PN5B896S; (**d**) 1PN5B898S and (**e**) STN5B880S.

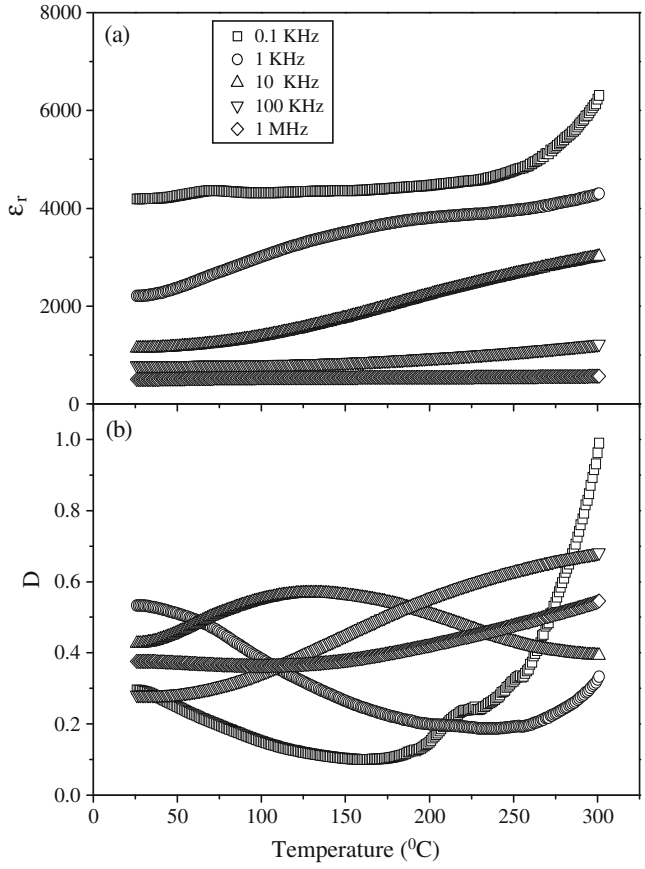


**Figure 8.** Variation of (**a**) dielectric constant, \g(e)\-(r) and (**b**) dissipation factor, *D*, with temperature at different frequencies for glass–ceramic sample 1PN5B898S.

relaxation time decreases with increasing temperature. This leads to increase in the peak temperature with increasing frequency of measurement. Due to the space charge relaxation processes, a maxima is observed in their dissipation factor, *D* vs *T* plots, whose position shifts to higher frequency with increasing temperature. The rise in the value of dielectric constant at 0·1 kHz may be due to the movement of alkali and alkaline earth ions at higher temperature which are present in the residual glass.

## 4. Conclusions

DTA patterns of the Pb-rich glass samples show more than one exothermic peak while DTA patterns of the Sr-rich glass show only one or two exothermic peaks. By spectroscopic study, it is concluded that the main groups of broad band such as $BO_3$ and $BO_4$ act as network modifier in the glassy matrix, while PbO and SrO appear in interstitial positions and $BO_4$ units increase with an increase in PbO for SrO content. It is also concluded that IR spectra of glass samples PTN5B, 9PN5B, 8PN5B, 7PN5B and 6PN5B, which are rich in PbO content, the absorption bands are shifted to lower wavenumber side. All the absorption peaks of IR pattern are well in agreement with standard data as given in table 2.

Eventually, we concluded that the studies on DTA and IR showed shifting in the peaks with replacement of PbO for SrO. XRD studies confirm the desired phase formation of PST/ST along with trace amount of secondary phases 'R' and 'SB'. SEM shows well developed and interconnected crystallites of major phase dispersed in the residual glassy matrix. High value of dielectric constant, $\varepsilon_r$ and low dissipation factor, $D$, were present due to the effect of addition of 1 mol% of $Nb_2O_5$.

## Acknowledgement

Authors are highly thankful to DRDO, India, for financial support to carry out research work at the Department of Ceramic Engineering, Institute of Technology, Banaras Hindu University, Varanasi.

## References

Adams R V and Douglas R W 1959 *J. Soc. Glass Tech.* **43** 147

Bray P G and Keefe J G O 1963 *J. Phys. Chem. Glasses* **4** 37

Bray P G, Leventhal M and Hooper H O 1963 *Phys. Chem. Glasses* **4** 47

Chekhovskii V G 1985 *Fisika I Khimiya stekla* **11** 24 (Engl. Transl.)

Doweider H, Zeid M A A and El-Damrawi G M 1991 *J. Phys. D: Appl. Phys.* **24** 2222

Dunken H and Doremus R H 1987 *J. Non-Cryst. Solids* **92** 61

Ezz Eldin F M, Alaily N A E L, Khalifa F A and Batal H A E L 1995 *Fundamentals of glass science and technology*, in *Proc. 3rd E.S.G. conf.* (Germany: Verlag Der Deutschen Glastechnischen Gesselschaft)

Gautam C R 2005 *Study of crystallization, microstructure and electrical behaviour of lead strontium titanate borosilicate glass–ceramics with $La_2O_3$ and $Nb_2O_5$ as additives*, Ph.D. Thesis (Varanasi: Banaras Hindu University)

Gautam C R, Kumar D and Parkash O 2010 *Bull. Mater. Sci.* **33** 145

Gautam C R, Kumar D and Parkash O 2011a *Adv. Mater. Sci. Eng.* **2011** 1

Gautam C R, Kumar D and Parkash O 2011b *Bull. Mater. Sci.* **34** 1

Ghoneun N A, Batal H A E I, Abdel Shafi N and Azooz M H 1996 *Proceedings of Egyptian Conference of Chemistry*, *Cairo, Egypt* **162**

Hirashima H, Arari D and Yoshida T 1985 *J. Am. Ceram. Soc.* **68** 486

Husung R H and Doremus R H 1990 *J. Mater. Res.* **5** 2209

Kamitos E I and Karakassides M A 1989 *Phys. Chem. Glasses* **30** 19

Kamitos E I, Karakassides M A and Chryssikos G D 1987 *J. Phys. Chem. Glasses* **91** 1073

Keith H D and Padden F J 1963 *J. Appl. Sci.* **34** 2409

Khanna A, Bhatti S S, Singh K J and Thind K S 1996 *Nucl. Instrum. Meth.* **B114** 217

Kumar R V, Veeraiah N and Buddudu S 1997 *J. Phys.* **70** 951

Motke S G, Yawale S P and Yawale S S 2002 *Bull. Mater. Sci.* **25** 75

Rajendran V, Palanivelu N, El-Batal H A, Khalifa F A and Shafi N A 1999 *Acoust. Lett.* **23** 113

Sahu A K, Kumar D and Parkash O 2003a *Br. Ceram. Trans.* **102** 139

Sahu A K, Kumar D, Parkash O and Prakash C 2003b *Ceram. Int.* **30** 477

Sahu A K, Kumar D and Parkash O 2006 *J. Mater. Sci.* **41** 2075

Singh D, Singh K, Singh G, Manupriya, Mohan S and Arora M 2008 *J. Phys: Condens. Matter* **20** 75228

Singh K, Singh H, Sharma V, Nathuram R, Khanna A, Kumar R, Bhatti S S and Sahota H S 2002 *Nucl. Instrum. Meth.* **B194** 1

Singh S, Singh A P and Bhatti S S 1989 *J. Mater. Sci.* **24** 1539

Tenny A S and Wong J 1972 *J. Chem. Phys.* **56** 5516

Thakur O P, Kumar D, Parkash O and Pandey L 1997 *Bull. Mater. Sci.* **20** 67

Worrel C A and Henshell J 1978 *J. Non-Cryst. Solids* **29** 283